Editors' Suggestion

Dissipative Parametric Gain in a GaAs/AlGaAs Superlattice

Vladislovas Čižas,[1] Liudvikas Subačius,[1] Natalia V. Alexeeva,[1] Dalius Seliuta,[1] Timo Hyart,[2,3] Klaus Köhler,[4] Kirill N. Alekseev,[1,5,*] and Gintaras Valušis[1,6,†]

[1]*Department of Optoelectronics, Center for Physical Sciences and Technology, Saulėtekio Avenue 3, LT-10257 Vilnius, Lithuania*

[2]*International Research Centre MagTop, Institute of Physics, Polish Academy of Sciences, Avenue Lotników 32/46, 02-668 Warsaw, Poland*

[3]*Department of Applied Physics, Aalto University, 00076 Aalto, Espoo, Finland*

[4]*Fraunhofer-Institut für Angewandte Festkörperphysik, Tullastrasse 72, Freiburg D-79108, Germany*

[5]*Department of Physics, Loughborough University, Loughborough LE11 3TU, United Kingdom*

[6]*Institute of Photonics and Nanotechnology, Department of Physics, Vilnius University, Saulėtekio Ave. 3, LT-10257 Vilnius, Lithuania*

(Received 16 November 2021; accepted 4 May 2022; published 8 June 2022)

Parametric generation of oscillations and waves is a paradigm, which is known to be realized in various physical systems. Unique properties of quantum semiconductor superlattices allow us to investigate high-frequency phenomena induced by the Bragg reflections and negative differential velocity of the miniband electrons. Effects of parametric gain in the superlattices at different strengths of dissipation have been earlier discussed in a number of theoretical works, but their experimental demonstrations are so far absent. Here, we report on the first observation of the dissipative parametric generation in a subcritically doped GaAs/AlGaAs superlattice subjected to a dc bias and a microwave pump. We argue that the dissipative parametric mechanism originates from a periodic variation of the negative differential velocity. It enforces excitation of slow electrostatic waves in the superlattice that provide a significant enhancement of the gain coefficient. This work paves the way for a development of a miniature solid-state parametric generator of GHz-THz frequencies operating at room temperature.

DOI: 10.1103/PhysRevLett.128.236802

Introduction.—Parametric generation is a paradigm, known to be realized in various physical systems ranging from electronic circuits and nonlinear optics to modern optomechanical and Josephson mesoscopic devices for quantum information processing [1–3]. A large pump tone of the frequency ω_0 causes a periodic variation of a reactive element, which through mechanism of parametric resonance results in the degenerate $2\omega_1 = \omega_0$ or nondegenerate $\omega_1 + \omega_2 = \omega_0$ processes of regenerative amplification, and thus both modes 1 and 2 can self-oscillate [4,5]. Positive gain can also be reached in the phase-sensitive process of frequency up-conversion $\omega_2 + \omega_0 = \omega_1$, but such amplification is not regenerative and instead is governed by the familiar Manley-Rowe relations for powers associated with each of the modes [6].

However, there also exists a lesser known dissipative parametric mechanism associated with a periodic variation of a nonlinear resistance, and it is often responsible for the generation of subharmonics in electric circuits modeled by driven nonlinear oscillators [7]. This mechanism requires that the system visits the state of negative differential resistance during part of the ac pump period [7,8]. In the case of several modes, electric powers associated with every frequency are connected by the Pantell relations, which explicitly involve the differential conductance of nonlinear resistive circuits [9].

Quantum semiconductor superlattices (SLs) [10] can be found as a unique platform to meet the aforesaid condition. In these artificial crystals, miniband electrons can perform electrically driven high-frequency oscillations caused by the Bragg reflections [11]. The major focus is on the dc field induced Bloch oscillations, detectable both in time [12] and in space [13], and on the related dissipative phenomenon of Bloch gain [14]. The electron drift velocity (v) depends on the electric field following a nonlinear curve that above a certain critical field (E_{cr}) demonstrates the negative differential velocity (NDV) [10,15]. This active Esaki-Tsu nonlinearity is able to provide an efficient multiplication of the microwave input frequency in SL-based devices [16]. It was a significant progress to realize such THz frequency multipliers and mixers experimentally and obtain reasonable power output suitable for various applications [17–19].

Theories of parametric amplification and generation of high frequencies in quantum SLs exist for more than 40 yr [20–29], and include, along with the earlier contributions [20–22], the thorough analysis of the degenerate [23,24], nondegenerate [25], and multifrequency [26] parametric processes. Overall, the amplification is caused by the electronic Bragg reflections in the narrow energy band; it was predicted to be multiphoton and to exist for a very wide range of the pump frequencies (ω_0) that cover significant parts of GHz and THz frequency domains [23]. Nevertheless, microscopic physical mechanisms behind the parametric gain were found to be distinct whether $\omega_0\tau > 1$ or $\omega_0\tau \ll 1$ ($\tau \simeq 200$ fs is a characteristic relaxation time at room temperature [14,17]). In the case of high-frequency pump $\omega_0\tau > 1$, the parametric gain has its origin in a periodic variation of the effective electron mass and specific kinetic inductance of the miniband electrons [23,27]. Furthermore, in the limit of small dissipation ($\omega_0\tau \gg 1$), the Manley-Rowe relations are satisfied [25].

The behavior is quite different in the limit of strong dissipation ($\omega_0\tau \ll 1$), which corresponds to GHz pump frequencies [25,28,29]. Now not only the down-conversion but also the up-conversion process can provide regenerative amplification [22,25]. This dissipative parametric gain in SLs [25,28,29], while being in essence similar to that in nonlinear resistors, still relies on a periodic switching to the NDV state rather than on negative values of the differential conductance as in Ref. [9]. Indeed, an account of space charge effects in the basic transport model reveals that the static differential conductance of the moderately doped quantum SL is always positive [30], in agreement with the earlier findings [31,32]. Despite decades of fruitful theoretical developments, there was no experimental evidence of the parametric gain effects in SLs so far.

In this Letter, we report on the first experimental observation of the dissipative parametric generation in a SL device subjected to a dc bias and a microwave pump. We detect both the degenerate and nondegenerate multiphoton parametric processes, together with signatures of large-signal gain effects. In this room temperature experiment, we use a special design of the device composed of a wide miniband GaAs/AlGaAs SL with asymmetric non-Ohmic contacts, allowing to make the electric field profile within the active part of the structure more uniform. We find that net optical gain for this parametric device can be almost a thousand times greater than follows from the earlier estimate [23], and argue that the enhancement originates from slow propagation of the intrinsic electrostatic waves inside the SL [33].

Superlattice design and characterization.—Experiments were performed using the GaAs/AlGaAs SL structure given in Fig. 1(a). It contains 30 periods of 5 nm GaAs: Si quantum wells (10^{16} cm^{-3}) separated by 1 nm $Al_{0.3}Ga_{0.7}As$ barriers to enable a wide miniband of 104 meV. The AuTi Schottky contact was fabricated on top of the structure, while from the SL bottom, the

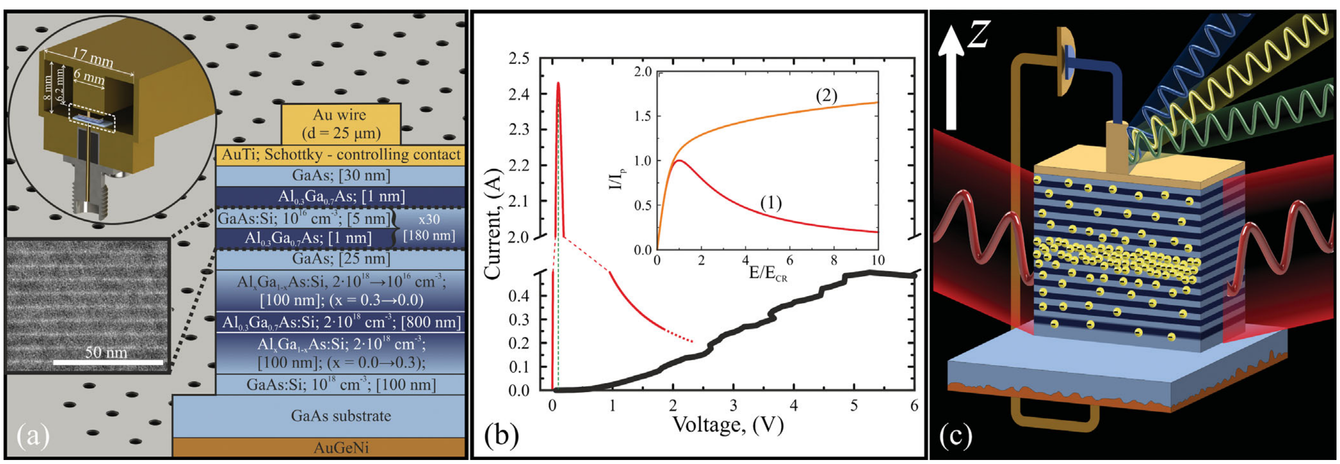

FIG. 1. (a) Architecture of the GaAs/AlGaAs device where SL sandwiched between the AuTi Schottky contact from the top and the heterojunction from the bottom. To deliver the incident microwave to the structure, it was placed along the wide wall of a single-ridged waveguide of 17×8 mm. Inset: TEM image of the superlattice. (b) The measured *I-V* characteristic of the SL device (thick black) in comparison with the ideal Esaki-Tsu *I-V* characteristic (thin red). The vertical (dashed green) line marks the critical voltage ($E_{\mathrm{cr}}L \approx 0.1$ V), for which the peak current $I_p \approx 2.4$ A is reached. Inset: The Esaki-Tsu curve (1, red) versus the calculated *I-V* characteristic of SL with Ohmic injecting contact (2, orange). Notice that the experimental *I-V* curve runs significantly below I_p, which is opposite to the behavior of *I-V* characteristics in the case of Ohmic contacts. This points to non-Ohmic nature of contacts in our SL device. (c) Sketch of the parametric generation in the SL device. Strong electromagnetic wave is coupled with electron plasma of the dc biased SL. The electric field component of this pump wave, directed along the SL axis z, parametrically interacts with the miniband electrons and excites a dozen of growing waves at frequencies satisfying the parametric conservation relations for photons [Eq. (1)]. The generated longitudinal electrostatic waves propagate along z at the electron drift velocity before being converted to radiation through the wire antenna. Spatial modulation of the electron density associated with only one of such slow waves is shown schematically.

GaAs/AlGaAs heterojunction was formed. The SL processed into a square mesa of 80×80 μm dimensions and of 1.3 μm height using wet etching was then mounted inside the standard single-ridged waveguide. The gold wire of $\simeq 25$ μm was attached to the top contact of the SL to ensure proper coupling to microwaves and to serve for biasing of the structure. The bottom Ohmic contact was connected to the coaxial line via filter. Measurements were performed employing a waveguide-based setup [34] relying on changes in the microwave transmission and reflection induced by the electron transport in the SL [35].

For this SL the product of the doping density $N = 10^{16}$ cm^{-3} and the length $L = 180$ nm is below the specific critical value determining the onset of the traveling high-field domains, $(NL)_{\mathrm{cr}} = 7\epsilon E_{\mathrm{cr}}/e = 2.7 \times 10^{11}$ cm^{-2} [35,38,44]. Therefore, our subcritically doped SL operates in the electrically stable transport regime [45], in a similar way to the well-known experiments [14,46].

The experimental *I-V* characteristic of the SL device, measured employing electrical pulses of 20 ns duration, is presented in Fig. 1(b). It has positive slope, which is a typical feature of electronic systems with NDV operating in the stable transport regime [30,32,47]. By taking this for granted, we find how a comparison of the experimental and so-called neutral *I-V* characteristics can be used to extract information on the nature of electric contacts of the SL. The neutral characteristic references to a special situation of the electric neutrality, when densities of the mobile and fixed (N) charges coincide, electric field is homogeneous, and contacts are absent [47]. In our case, this is the ideal Esaki-Tsu *I-V* characteristic, the shape of which directly follows the $v(E)$ dependence. Next, both the calculations [30] and the experiments [14,46] expose that *I-V* characteristics of SLs with Ohmic contacts typically saturate either above the Esaki-Tsu peak current I_p [Fig. 1(b) inset] or on the level of I_p (inset of Fig. 1 in Ref. [14]). On the contrary, the measured *I-V* characteristic runs significantly below I_p [Fig. 1(b)], indicating the non-Ohmic nature of contacts in our device. We attribute this non-Ohmicity to the presence of Schottky and shallow heterojunction barriers. Typically, the use of non-Ohmic contacts in NDV devices makes the electric field profile more uniform, and thus contributes to the better performance [47,48]. In addition, the built-in voltage of 0.65 V increases the voltage drop across the SL by this amount.

Experimental results and discussion.—Our experiment on the parametric generation in the SL device is sketched in Fig. 1(c). A strong electromagnetic wave passes through the SL along its layers, modulates the electron differential velocity, and by means of the dissipative parametric mechanism excites a spectrally rich coherent emission from the device into the output waveguide. In the earlier theoretical suggestions, the generated spectral components were assumed to be transverse electromagnetic modes of the external cavity (cf. Fig. 1 in Ref. [23]). Contrastingly,

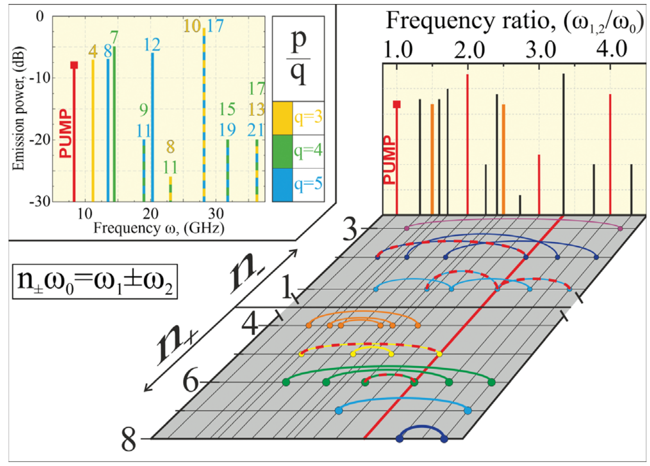

FIG. 2. The spectrum of the frequencies generated in SL under the action 8.45 GHz pump and bias of 0.3 V. The frequencies are scaled to the pump frequency (vertical panel). The spectral lines corresponding to the pump and its multiplication (red), the half-harmonics (orange), and to the nondegenerate parametric processes (black) are displayed. The $1/2$ harmonic is not visible due to cutoff characteristics of the output waveguide. The links in the horizontal panel indicate that the observed emission lines follow the spectrum of the small-signal parametric gain [Eq. (1)]. Multiphoton and multiple wave mixing phenomena (red dashed lines), related to the generation at 28.20 GHz (horizontal solid red line), are further exemplified in Eqs. (2). Inset: The frequencies classified according to the pump fractions [Eq. (3)]. The corresponding numerators p are shown nearby their spectral lines, while the denominators q are defined following the color chart.

our device operates without such resonator and mainly relies on intrinsic longitudinal modes inside the SL that are growing from fluctuations of the electron plasma. We will return to the discussion of the origin and significance of these intrinsic modes after consideration of the generated frequencies in light of the major predictions of the theory.

The measured emission spectrum for the case of 8.45 GHz pump is presented in Fig. 2 (vertical panel). The strength of ac field inside the SL was estimated to be $\simeq 8E_{\mathrm{cr}}$ [35]. Along with the pump and its harmonics up to the 4th order, the spectrum also contains additional 11 emission lines. The prerequisite for an enforcement of the stimulated emission at these discrete frequencies is a positive gain for infinitesimal signals. The theory states that the small-signal parametric gain in SLs can arise only for the frequencies $\omega_{1,2}$ that are connected to the pump frequency as

$$\omega_1 \pm \omega_2 = n_\pm \omega_0, \qquad 2\omega_1 = n_0 \omega_0, \tag{1}$$

where n_+, n_- are positive integers and n_0 is odd [23,25,29]. The existence of the parametric relations with $n \neq 1$ is a definitely notable property of the quantum superlattice nonlinearity. Whereas generation of the half-harmonics and spontaneous down-conversions with various n_+ are universal signatures of the parametric gain in SLs [23], the appearance of self-oscillations at both frequencies involved in the up-conversion processes (cf. Fig. 2 and tables in Ref. [35]) [Eq. (1) with $n_- \geq 1$] is a remarkable property of the dissipative mechanism [22,25].

The data and links displayed in Fig. 2 affirm that the observed parametric emission lines (black and orange) satisfy the photon energy conservation relations of Eqs. (1), and thus can include many photons of the pump ($n > 1$). Surprisingly, we also found that almost every spectral line participates in several multiphoton processes simultaneously. For instance, the frequency 28.20 GHz is generated in the following processes (cf. Fig. 2 and Ref. [35]):

$$\begin{cases} \mathbf{28.20} + 23.05 = 6 \times 8.45\ \text{GHz}\ (8\,\text{photons}), \\ \mathbf{28.20} + 13.45 = 5 \times 8.45\ \text{GHz}\ (7\,\text{photons}), \\ \mathbf{28.20} - 11.20 = 2 \times 8.45\ \text{GHz}\ (4\,\text{photons}), \\ \mathbf{28.20} - 20.30 = 1 \times 8.45\ \text{GHz}\ (3\,\text{photons}), \\ 36.25 - \mathbf{28.20} = 1 \times 8.45\ \text{GHz}\ (3\,\text{photons}). \end{cases} \quad (2)$$

This unusual behavior in SLs is in sharp contrast to the parametric generation in conventional optical systems, where multiphoton effects involving the pump ($n\hbar\omega_0$) are virtually absent, and even multistep frequency cascades [49] are well described by the Manley-Rowe relations [50,51]. As a consequence, optical parametric generation of the frequencies involved in the up-conversion processes with several pump photons ($n_- = 2, 3$) is unlikely realizable [51], but such emission lines are readily observable in the SL, see Fig. 2.

Furthermore, the measured emission spectrum can bear signatures of generation effects that go beyond the linear response in signal strengths. In the case of large signals ($\simeq E_{\rm cr}$), it is predicted that new channels in parametric generation induce the fractional frequencies

$$\omega_1 = (p/q)\omega_0, \quad q > 2, \quad (3)$$

where p, q are integers [24,26]. In particular, the subharmonics $p\omega_0/3$ and $p\omega_0/4$ can arise due to effects that are quadratic and cubic in the signal strength, respectively [24]. Analysis of the data (Fig. 2 inset) unveils this type of frequencies and thus experimentally confirms involvement in the large signal regime. Similar emission spectra, the spectral components of which do fit Eqs. (1) and (3), were observed for other pump frequencies close to 10 GHz. Different multiphoton parametric processes in SL can be also distinguished by comparing their input-output power dependencies [35]. At the present state of the art, however, this method is less informative than the used spectroscopic approach.

Theoretical justification.—To get deeper insight into the role of the observed multiple simultaneous parametric processes, we calculate and compare the high-frequency electron mobilities $\mu_n(E_{\rm dc}, E_0)$ for two processes with $n = 1$ and $n = 2$ separately [Eq. (1)], and also for their combination [cf. Eqs. (2)]. The total pump electric field was assumed to be the sum of dc bias $E_{\rm dc}$ and strong ac field $E_0 \cos(\omega_0 t)$, where $\omega_0 \tau \ll 1$ [35]. The calculated areas of gain ($\mu_n < 0$) and absorption ($\mu_n > 0$) in the plain $E_0 - E_{\rm dc}$ are presented in Fig. 3. For both single parametric processes shown in the subplots (a) and (b), there exist wide blank areas of no gain, which effectively can cause appearance and disappearance of the amplification at relatively large values of either E_0 or $E_{\rm dc}$. However, in the case the two parametric processes run simultaneously, the gain area expands and the blank area survives only for rather weak applied fields $\lesssim E_{\rm cr}$ [Fig. 3(c)]. This determines a well-defined threshold line for the positive gain when $E_0 \simeq E_{\rm dc} \simeq E_{\rm cr}$. Therefore, an account of the multiple processes in SLs restores intuitive correspondence with the condition of dissipative parametric amplification in nonlinear resistors.

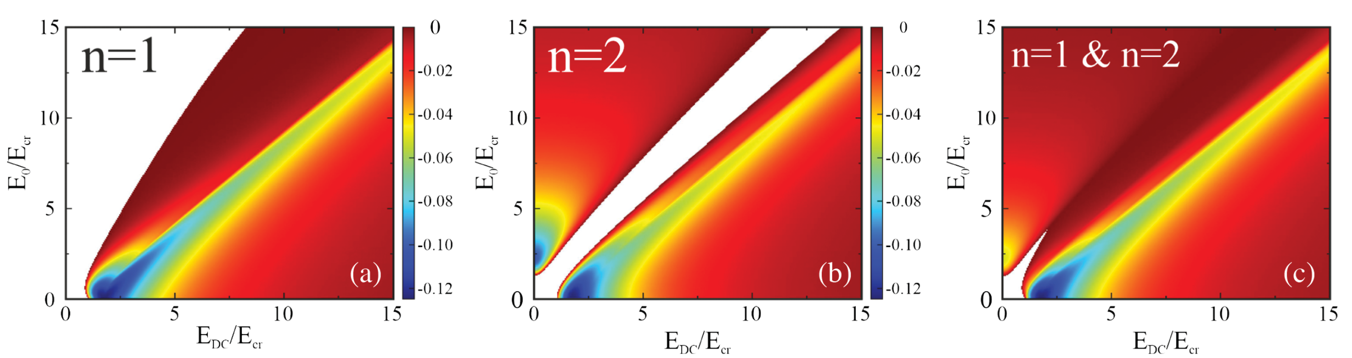

FIG. 3. (a)–(b) The areas and magnitudes of gain $\mu_n < 0$ (color) in the plane of dc bias $E_{\rm dc}$ and pump field amplitude E_0 for $n = 1$ (a) and $n = 2$ (b). The calculated high-frequency mobilities μ_n are presented in units of the superlattice Drude mobility $(2v_p/E_{\rm cr})$, and the dc and ac electric fields are scaled to the critical field $E_{\rm cr}$. Blank areas everywhere correspond to absorption ($\mu_n > 0$). (c) Overlapping of the areas corresponding to both $\mu_1 < 0$ and $\mu_2 < 0$ (color) in the same plane. The figure illustrates an overall extension of the gain area with the only boundary at low fields, in the case when two parametric processes are simultaneously realized in the SL.

We turn to the origin of the intrinsic electrostatic modes [Fig. 1(c)] and their contribution to the net optical gain. Generally, every such electrostatic mode propagates at the drift velocity of electrons [52], and represents an undamped excitation of the solid state plasma in condition of NDV [53]. Specifically for the Esaki-Tsu active nonlinearity, it is known as the drift-relaxation self-mode of SL [33] caused by the Bragg reflections of the miniband electrons [54]. We apply this concept to the case of the dissipative parametric gain.

Consider an intrinsic longitudinal mode which frequency satisfies one of the parametric relations of Eqs. (1) at some fixed photon number n. If the corresponding $\mu_n < 0$, in the linear stage small fluctuations of the electric field grow exponentially while electron flow propagates with the drift velocity v through the sample of the length L. The growth rate of the electrostatic wave is determined by the product of the dielectric relaxation frequency $(eN\mu_n)/\epsilon$ and the electron transit time L/v [55]. Therefore, the gain coefficient β_n, defined by means of the Beer law $I_{\rm out} = I_{\rm in}\exp(-\beta z)$, can be estimated as

$$\beta_n = \frac{2eN\mu_n}{\epsilon v}. \quad (4)$$

Remarkable, the direct substitution $v/2 \simeq v_p \to c'$ transforms the right-hand side of Eq. (4) into the corresponding gain coefficient of the electromagnetic mode traveling at the speed of light in the semiconductor $c' = c/n_r$ (n_r is the average refractive index of SL) [23,56]. Since the $v_p/c' \simeq 10^{-3}$ contribution of the slow electrostatic modes to the net optical gain can prevail. By assuming $\mu_1/\mu_0 \approx -0.02$ for the three-photon parametric processes [Fig. 3(a)] we obtain from Eq. (4) large gain $\beta_1 \gtrsim 10^4\ {\rm cm}^{-1}$ for the corresponding slow modes.

Finally, the generated electrostatic modes are transformed to the coherent electromagnetic radiation through a wire antenna bonded to the SL [Fig. 1(c)]. It is worth noticing that similar phase-preserving conversions of electromagnetic waves to plasmons and back have been demonstrated in nanometric field effect transistors [57,58].

Conclusion.—We observed and explained unusual parametric generation in a quantum optoelectronic system with strong dissipation when the Manley-Rowe relations are broken. We showed that intensive microwave pumping of the GaAs/AlGaAs superlattice stimulates dissipative parametric gain at room temperature, manifesting itself as a steady coherent emission at various fractional harmonics of the pump frequency. Unusually, this device starts to self-oscillate in up-conversion processes as easy as in down-conversion ones. We also revealed the significance of the undamped drift-relaxation modes for the amplification mechanism in the superlattice. These slow plasma waves can provide large gain of $\simeq 10^4\ {\rm cm}^{-1}$ and more, thus enabling multiphoton generation in the cavityless configuration. Our experiments confirmed core predictions of the existing theory of dissipative parametric amplification at GHz frequencies, and also further stretched its limits by describing the multiple parametric processes. At once, semiconductor quantum SLs hold the promise of room temperature parametric amplification in the technologically important sub-THz range and beyond [23].

We are sincerely grateful to Martynas Skapas, Sandra Stanionytė, and Remigijus Juškėnas for superlattice characterization; Linas Minkevičius, Vladimir Maksimenko, and Miron S. Kagan for illuminating discussions. The research activities of K. N. A. were partially funded by the Marius Jakulis Jason Foundation and T. H. was supported, in part, by the Foundation for Polish Science through the IRA Programme co-financed by the EU within SG OP.

*kirill.alekseev@ftmc.lt
†gintaras.valusis@ftmc.lt

[1] C. F. Ockeloen-Korppi, E. Damskägg, J. M. Pirkkalainen, T. T. Heikkilä, F. Massel, and M. A. Sillanpää, Low-Noise Amplification and Frequency Conversion with a Multiport Microwave Optomechanical Device, Phys. Rev. X **6**, 041024 (2016).

[2] W. Wustmann and V. Shumeiko, Parametric effects in circuit quantum electrodynamics, Low Temp. Phys. **45**, 848 (2019).

[3] Z. R. Lin, K. Inomata, K. Koshino, W. D. Oliver, Y. Nakamura, J. S. Tsai, and T. Yamamoto, Josephson parametric phase-locked oscillator and its application to dispersive readout of superconducting qubits, Nat. Commun. **5**, 4480 (2014).

[4] J. W. Strutt, On the intensity of light reflected from certain surfaces at nearly perpendicular incidence, Proc. R. Soc. **41**, 275 (1887).

[5] M. I. Rabinovich and D. I. Trubetskov, *Oscillations and Waves in Linear and Nonlinear Systems* (Springer, Netherlands, 1989).

[6] J. M. Manley and H. E. Rowe, Some general properties of nonlinear elements-part I. General energy relations, Proc. IRE **44**, 904 (1956).

[7] L. Mandelstam and N. Papalexi, Über Resonanzerscheinungen bei Frequenzteilung, Z. Phys. **73**, 223 (1932).

[8] V. V. Migulin, V. I. Medvedev, E. R. Mustel, and V. N. Parygin, *Basic Theory of Oscillations* (Mir Publishers, Moscow, 1989).

[9] R. H. Pantell, General power relationships for positive and negative nonlinear resistive elements, Proc. IRE **46**, 1910 (1958).

[10] L. Esaki and R. Tsu, Superlattice and negative differential conductivity in semiconductors, IBM J. Res. Dev. **14**, 61 (1970).

[11] F. Bass and A. Tetervov, High-frequency phenomena in semiconductor superlattices, Phys. Rep. **140**, 237 (1986).

[12] J. Feldmann, K. Leo, J. Shah, D. A. B. Miller, J. E. Cunningham, T. Meier, G. von Plessen, A. Schulze, P. Thomas, and S. Schmitt-Rink, Optical investigation of

Bloch oscillations in a semiconductor superlattice, Phys. Rev. B **46**, 7252 (1992).

[13] V. G. Lyssenko, G. Valušis, F. Löser, T. Hasche, K. Leo, M. M. Dignam, and K. Köhler, Direct Measurement of the Spatial Displacement of Bloch-Oscillating Electrons in Semiconductor Superlattices, Phys. Rev. Lett. **79**, 301 (1997).

[14] P. G. Savvidis, B. Kolasa, G. Lee, and S. J. Allen, Resonant Crossover of Terahertz Loss to the Gain of a Bloch Oscillating InAs/AlSb Superlattice, Phys. Rev. Lett. **92**, 196802 (2004).

[15] A. Sibille, J. F. Palmier, H. Wang, and F. Mollot, Observation of Esaki-Tsu Negative Differential Velocity in GaAs/AlAs Superlattices, Phys. Rev. Lett. **64**, 52 (1990).

[16] A. A. Ignatov and Y. A. Romanov, Nonlinear electromagnetic properties of semiconductors with a superlattice, Phys. Status Solidi B **73**, 327 (1976).

[17] K. F. Renk, B. I. Stahl, A. Rogl, T. Janzen, D. G. Pavel'ev, Y. I. Koshurinov, V. Ustinov, and A. Zhukov, Subterahertz Superlattice Parametric Oscillator, Phys. Rev. Lett. **95**, 126801 (2005).

[18] D. G. Paveliev, Y. I. Koshurinov, A. S. Ivanov, A. N. Panin, V. L. Vax, V. I. Gavrilenko, A. V. Antonov, V. M. Ustinov, and A. E. Zhukov, Experimental study of frequency multipliers based on a GaAs/AlAs semiconductor superlattices in the terahertz frequency range, Semiconductors **46**, 121 (2012).

[19] D. J. Hayton, A. Khudchenko, D. G. Pavelyev, J. N. Hovenier, A. Baryshev, J. R. Gao, T. Kao, Q. Hu, J. L. Reno, and V. Vaks, Phase locking of a 3.4 THz third-order distributed feedback quantum cascade laser using a room-temperature superlattice harmonic mixer, Appl. Phys. Lett. **103**, 051115 (2013).

[20] V. V. Pavlovich, Nonlinear amplification of electromagnetic waves in a semiconductor with a superlattice, Sov. Phys. Solid State **19**, 54 (1977).

[21] L. K. Orlov and Y. A. Romanov, Decay instability of electromagnetic waves in superlattices, Radiophys. Quantum Electron. **23**, 942 (1980).

[22] L. K. Orlov and Y. A. Romanov, Parametric mixing of electromagnetic waves in superlattices, Radiophys. Quantum Electron. **25**, 506 (1982).

[23] T. Hyart, A. V. Shorokhov, and K. N. Alekseev, Theory of Parametric Amplification in Superlattices, Phys. Rev. Lett. **98**, 220404 (2007).

[24] A. V. Shorokhov and K. N. Alekseev, Theoretical backgrounds of nonlinear THz spectroscopy of semiconductor superlattices, Int. J. Mod. Phys. B **23**, 4448 (2009).

[25] T. Hyart and K. N. Alekseev, Nondegenerate parametric amplification in superlattices and the limits of strong and weak dissipation, Int. J. Mod. Phys. B **23**, 4403 (2009).

[26] Y. A. Romanov and Y. Y. Romanova, Self-oscillations in semiconductor superlattices, J. Exp. Theor. Phys. **91**, 1033 (2000).

[27] T. Hyart, N. V. Alexeeva, A. Leppänen, and K. N. Alekseev, Terahertz parametric gain in semiconductor superlattices in the absence of electric domains, Appl. Phys. Lett. **89**, 132105 (2006).

[28] K. N. Alekseev, M. V. Gorkunov, N. V. Demarina, T. Hyart, N. V. Alexeeva, and A. V. Shorokhov, Suppressed absolute negative conductance and generation of high-frequency radiation in semiconductor superlattices, Europhys. Lett. **73**, 934 (2006).

[29] Y. A. Romanov, J. Y. Romanova, and L. G. Mourokh, Semiconductor superlattice in a biharmonic field: absolute negative conductivity and static electric-field generation, J. Appl. Phys. **99**, 013707 (2006).

[30] V. A. Maksimenko, V. V. Makarov, A. A. Koronovskii, A. E. Hramov, R. Venckevičius, G. Valušis, A. G. Balanov, F. V. Kusmartsev, and K. N. Alekseev, Electric-field distribution in a quantum superlattice with an injecting contact: Exact solution, JETP Lett. **103**, 465 (2016).

[31] W. Schockley, Negative resistance arising from transit time in semiconductor diodes, Bell Syst. Tech. J. **33**, 799 (1954).

[32] H. Kroemer, Generalized proof of Shockley's positive conductance theorem, Proc. IEEE **58**, 1844 (1970).

[33] A. A. Ignatov and V. I. Shashkin, Bloch oscillations of electrons and instability of space-charge waves in superconductor superlattices, Sov. Phys. JETP **66**, 526 (1987).

[34] L. Subačius, K. Jarašiūnas, P. Ščajev, and M. Kato, Development of a microwave photoconductance measurement technique for the study of carrier dynamics in highly-excited 4H-SiC, Meas. Sci. Technol. **26**, 125014 (2015).

[35] See Supplemental Material at http://link.aps.org/supplemental/10.1103/PhysRevLett.128.236802 for detailed description of the experimental setup, calculations of the HF mobilities, explanation of the NL criterion, estimation of the ac-field strength inside the structure, and input-output power dependencies. It also provides the data related to Fig. 2 in the form of tables and includes Refs. [14,28,34,36–43].

[36] Y. Y. Romanova, Parametric generation of high-frequency harmonics in semiconductor superlattices, Semiconductors **46**, 1451 (2012).

[37] A. V. Shorokhov and K. N. Alekseev, High-frequency absorption and gain in superlattices: Semiquasistatic approach, Physica (Amsterdam) **33E**, 284 (2006).

[38] A. A. Ignatov, V. I. Piskarev, and V. I. Shashkin, Instability (formation of domains) of an electric field in multilayer quantum structures, Sov. Phys. Semicond. **19**, 1345 (1985).

[39] B. Rieder, Semiclassical transport in semiconductor superlattices with boundaries, Ph. D. thesis, University of Regensburg, 2004.

[40] C. Wang, M. J. Burek, Z. Lin, H. A. Atikian, V. Venkataraman, I. Huang, P. Stark, and M. Lončar, Integrated high quality factor lithium niobate microdisk resonators, Opt. Express **22**, 30924 (2014).

[41] H. Zhao, Q An, X. Ye, B. H. Yu, Q. H. Zhang, F. Sun, Q. Y. Zhang, F. Yang, J. Guo, and J. Zhao., Second Harmonic Generation in AB-type $LaTiO_3/SrTiO_3$ Superlattices, Nano Energy **82**, 105752 (2021).

[42] Y. Du, S. N. Zhu, Y. Y. Zhu, P. Xu, C. Zhang, Y. B. Chen, Z. W. Liu, N. B. Minget, X. R. Zhang, F. F. Zhang, and S. Y. Zhang, Parametric and cascaded parametric interactions in a quasiperiodic optical superlattice, Appl. Phys. Lett. **81**, 1573 (2002).

[43] R. Byer, Quasi-phasematched nonlinear interactions and devices, J. Nonlinear Opt. Phys. Mater. **06**, 549 (1997).

[44] H. Kroemer, Theory of the Gunn effect, Proc. IEEE **52**, 1736 (1964).

[45] H. Kroemer, External negative conductance of a semiconductor with negative differential mobility, Proc. IEEE **53**, 1246 (1965).

[46] A. Sibille, J. F. Palmier, F. Mollot, H. Wang, and J. C. Esnault, Negative differential conductance in GaAs/AlAs superlattices, Phys. Rev. B **39**, 6272 (1989).

[47] D. Dascălu, *Transient-Time Effects in Unipolar Solid-State Devices* (Abacus Press, Kent, UK, 1974).

[48] S. P. Yu, W. Tantraporn, and J. Young, Transit-time negative conductance in GaAs bulk-effect diodes, IEEE Trans. Electron Devices **18**, 88 (1971).

[49] R. A. Andrews, H. Rabin, and C. L. Tang, Coupled Parametric Downconversion and Upconversion with Simultaneous Phase Matching, Phys. Rev. Lett. **25**, 902 (1970).

[50] A. S. Chirkin, V. V. Volkov, G. D. Laptev, and E. Y. Morozov, Consecutive three-wave interactions in nonlinear optics of periodically inhomogeneous media, Quantum Electron. **30**, 847 (2000).

[51] S. M. Saltiel, A. A. Sukhorukov, and Y. S. Kivshar, *Multistep Parametric Processes in Nonlinear Optics*, edited by E. Wolf, Progress in Optics Vol. 47 (Elsevier, New York, 2005), pp. 1–73.

[52] M. A. Lampert, Plasma oscillations at extremely high frequencies, J. Appl. Phys. **27**, 5 (1956).

[53] E. Schöll, *Nonequilibrium Phase Transitions in Semiconductors* (Springer, New York, 1987).

[54] M. Büttiker and H. Thomas, Current Instability and Domain Propagation Due to Bragg Scattering, Phys. Rev. Lett. **38**, 78 (1977).

[55] W. Heinle, Principles of a phenomenological theory of Gunn-effect domain dynamics, Solid-State Electron. **11**, 583 (1968).

[56] A. Wacker, Gain in quantum cascade lasers and superlattices: A quantum transport theory, Phys. Rev. B **66**, 085326 (2002).

[57] C. Drexler, N. Dyakonova, P. Olbrich, J. Karch, M. Schafberger, K. Karpierz, Y. Mityagin, M. B. Lifshits, F. Teppe, O. Klimenko *et al.*, Helicity sensitive terahertz radiation detection by field effect transistors, J. Appl. Phys. **111**, 124504 (2012).

[58] Y. Matyushkin, S. Danilov, M. Moskotin, V. Belosevich, N. Kaurova, M. Rybin, E. D. Obraztsova, G. Fedorov, I. Gorbenko, V. Kachorovskii, and S. Ganichev, Helicity-sensitive plasmonic terahertz interferometer, Nano Lett. **20**, 7296 (2020).